

Syntheses, Structures, Spectroscopic Properties, and Thermal Behavior of Nickel(II) Mixed-Ligand Complexes with *N*,*N*,*N*′,*N*′-Tetramethylethylenediamine, Benzoylacetonate, and a Halide Anion

Keiko Miyamoto, Mariko Sakamoto, Chikashi Tanaka,[1] Ernst Horn,[1] and Yutaka Fukuda*

Department of Chemistry, Faculty of Science, Ochanomizu University,
2-1-1 Otsuka, Bunkyo-ku, Tokyo 112-8610

[1]Department of Chemistry, Faculty of Science, Rikkyo (St. Paul's) University,
3-34-1 Nishi-Ikebukuro, Toshima-ku, Tokyo 171-8501

Received December 9, 2004; E-mail: fukuda@cc.ocha.ac.jp

A series of nickel(II) complexes comprising *N*,*N*,*N*′,*N*′-tetramethylethylenediamine (tmen), benzoylacetonate (bzac), and a halide anion (X), Ni(tmen)(bzac)X·*n*(H_2O)(n = 1–4, X = Cl, Br, I), have been synthesized. A crystallographic study revealed that the chloride anion coordinates to the central metal, while bromide and iodide anions are located in the outer coordination sphere as the counter anion; the metal has a slightly distorted octahedral geometry, and the two monodentate ligands (aqua and chloro) are in the cis-position. In bromide and iodide complexes, having two water molecules of crystallization, a ladder-like hydrogen bond network is formed among halide anions, aqua ligands, and water of crystallization. In a chloride complex having no water of crystallization, a dimer is formed by strong intermolecular hydrogen bonding between the aqua ligand and the chloro and the benzoylacetonate ligands of the neighboring molecule. The behaviors of the complexes in solution vary, depending on the nature of the solvents, including deaquation and disproportionation, causing contrasting color changes of the solutions. The presence of a proposed intermediate in the disproportionation reaction, namely a 5-coordinated complex, was confirmed. Thermal gravimetric analysis suggests that these complexes lose water of crystallization, undergo deaquation–anation, and then lose the coordinated water before disproportionation into two ternary complexes.

One of our research focuses has been on the chromotropic behavior of inorganic complexes of transition metals, such as Ni(II) and Cu(II). In particular, nickel(II) complexes are known with a six-coordinate octahedral configuration, with five-coordinate square pyramidal or trigonal bi-pyramidal structures, and with four-coordinate square planar or tetrahedral configurations. It is a peculiarity of nickel(II)'s chemistry that complexes of one configuration can be easily converted to other configurations, usually accompanied by very contrasting color changes.[1] Due to this chromotropic behavior, Ni and Cu complexes can be expected to have such applications as thermosensitive coloring matters, various sensors (vapor sensor for organic solvents or humidity sensor) or Lewis-acid–base indicator, as well as, imaging materials.[2] In the past, various mixed-ligand nickel(II) and copper(II) complexes having chromotropic properties have been reported,[3–5] but most of those color changes were based on a change of the coordination mode between Sp (square planar) and Oh (octahedral) configurations. On the other hand, Hoshino et al., found an interesting disproportionation phenomenon of 6-coordinate Nickel(II) mixed-ligand complexes with *N*,*N*,*N*′,*N*′-tetramethylethylenediamine (tmen), acetylacetonate (acac), and halide anion X (X = Cl, Br, and I).[6] The complex, Ni(tmen)(acac)(H_2O)X, upon heating, or when dissolved in an organic solvent, turns into two Nickel(II) mixed-ligand complexes, namely [NiX_2-(tmen)] (Td = tetrahedral) and [Ni(acac)$_2$(tmen)] (Oh). Since then, no further study has been done on this peculiar phenomenon, except for related work by Saito et al., who conducted a study on a series of mixed-ligand nickel(II) bis-diketonato complexes, [Ni(β-dike)$_2$(diam)], namely one of the products resulting from the above-mentioned disproportionation.[7] They found that these bis-diketonate ternary complexes are all highly volatile and highly soluble in non-polar solvents. Having been interested in this disproportionation reaction, wherein we can observe a rather unique color change of the Nickel(II) complex between Td and Oh, we employed a different β-diketonate ligand having an aromatic substituent, and synthesized a new series of Nickel(II) mixed-ligand complexes, i.e. Ni(tmen)(bzac)X·*n*(H_2O) (X = Cl, Br, I, n = 1–4). Here, we report on their crystallographic structures and their behaviors in the solid state and in solutions. Interestingly, the bis-diketonate ternary complex resulting from the disproportionation of this series of complexes turned out to be nonvolatile.

Results and Discussion

Crystal Structure of Compounds Ni(tmen)(bzac)-X·*n*(H_2O). The crystal and molecular structures of [NiCl-(bzac)(tmen)(H_2O)] (**1**) and [Ni(bzac)(tmen)(H_2O)$_2$]X·2H_2O (X = Br or I) (**2** and **3**) were determined by X-ray analysis.[8] The molecular geometry and the non-hydrogen atom labelling scheme for these complexes are shown in Fig. 1, and selected bond distances and angles are listed in Table 1. X-ray crystallography revealed that the bromide **2** and the iodide **3** complexes are isomorphous and isostructural, comprising two wa-

Published on the web June 6, 2005; DOI 10.1246/bcsj.78.1061

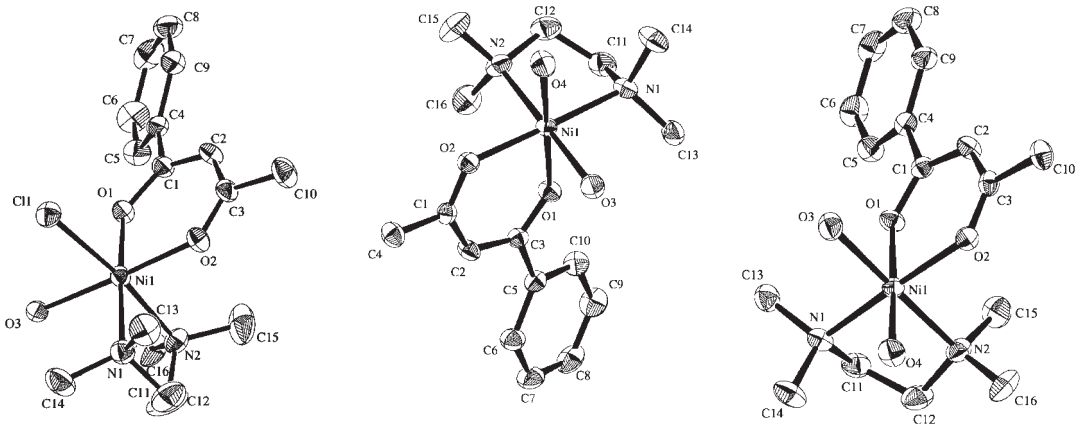

Fig. 1. ORTEP drawings of [NiCl(bzac)(tmen)(H_2O)] (**1**) (left), [Ni(bzac)(tmen)(H_2O)$_2$]Br·2H_2O (**2**) (center), and [Ni(bzac)(tmen)(H_2O)$_2$]I·2H_2O (**3**) (right). Hydrogen atoms counter anions and water of crystallization are omitted for clarity. Displacement ellipsoids are drawn at 30% probability.

Table 1. Selected Bond Distances (Å) and Angles (deg) for Ni(tmen)(bzac)X·$n$$H_2O$ (n = 1–4, X = Cl, Br, I)

[NiCl(bzac)(tmen)(H_2O)]					
Ni(1)–Cl(1)	2.465(2)	Ni(1)–O(1)	2.032(3)	Ni(1)–O(2)	2.015(3)
Ni(1)–O(3)	2.122(3)	Ni(1)–N(1)	2.195(4)	Ni(1)–N(2)	2.191(5)
Cl(1)–Ni(1)–O(1)	94.0(1)	Cl(1)–Ni(1)–O(2)	93.2(1)	Cl(1)–Ni(1)–O(3)	85.6(1)
Cl(1)–Ni(1)–N(1)	91.7(1)	Cl(1)–Ni(1)–N(2)	172.8(1)	O(1)–Ni(1)–O(2)	90.9(1)
O(1)–Ni(1)–O(3)	87.4(1)	O(1)–Ni(1)–N(1)	174.2(2)	O(1)–Ni(1)–N(2)	90.7(2)
O(2)–Ni(1)–O(3)	177.9(2)	O(2)–Ni(1)–N(1)	89.3(2)	O(2)–Ni(1)–N(2)	92.1(2)
O(3)–Ni(1)–N(1)	92.4(2)	O(3)–Ni(1)–N(2)	89.2(2)	N(1)–Ni(1)–N(2)	83.5(2)
[Ni(bzac)(tmen)(H_2O)$_2$]Br·2H_2O					
Ni(1)–O(1)	2.012(2)	Ni(1)–O(2)	2.039(2)	Ni(1)–O(3)	2.081(3)
Ni(1)–O(4)	2.117(3)	Ni(1)–N(1)	2.146(3)	Ni(1)–N(2)	2.161(3)
O(1)–Ni(1)–O(2)	89.31(9)	O(1)–Ni(1)–O(3)	86.9(1)	O(1)–Ni(1)–O(4)	176.1(1)
O(1)–Ni(1)–N(1)	88.5(1)	O(1)–Ni(1)–N(2)	92.7(1)	O(2)–Ni(1)–O(3)	88.3(1)
O(2)–Ni(1)–O(4)	88.7(1)	O(2)–Ni(1)–N(1)	175.8(1)	O(2)–Ni(1)–N(2)	91.8(1)
O(3)–Ni(1)–O(4)	89.8(1)	O(3)–Ni(1)–N(1)	95.2(1)	O(3)–Ni(1)–N(2)	179.6(1)
O(4)–Ni(1)–N(1)	93.7(1)	O(4)–Ni(1)–N(2)	90.6(1)	N(1)–Ni(1)–N(2)	84.8(1)
[Ni(bzac)(tmen)(H_2O)$_2$]I·2H_2O					
Ni(1)–O(1)	2.005(3)	Ni(1)–O(2)	2.036(3)	Ni(1)–O(3)	2.086(4)
Ni(1)–O(4)	2.119(3)	Ni(1)–N(1)	2.138(4)	Ni(1)–N(2)	2.155(4)
O(1)–Ni(1)–O(2)	89.6(1)	O(1)–Ni(1)–O(3)	87.1(1)	O(1)–Ni(1)–O(4)	176.0(1)
O(1)–Ni(1)–N(1)	88.4(1)	O(1)–Ni(1)–N(2)	93.0(1)	O(2)–Ni(1)–O(3)	87.8(1)
O(2)–Ni(1)–O(4)	89.1(1)	O(2)–Ni(1)–N(1)	175.8(1)	O(2)–Ni(1)–N(2)	91.8(1)
O(3)–Ni(1)–O(4)	89.1(2)	O(3)–Ni(1)–N(1)	95.8(2)	O(3)–Ni(1)–N(2)	179.6(2)
O(4)–Ni(1)–N(1)	93.2(1)	O(4)–Ni(1)–N(2)	90.8(2)	N(1)–Ni(1)–N(2)	84.6(2)

ter molecules of crystallization, one halide anion as the counter ion and a mononuclear complex unit consisting of a central nickel(II) cation, *N*,*N*,*N*′,*N*′-tetramethylethylenediamine, benzoylacetonate, and two aqua ligands. The central nickel(II) cation is coordinated by two nitrogen atoms of the tmen ligand, two oxygen atoms of the bzac ligand and two oxygen atoms of two aqua ligands, to give a slightly distorted octahedral geometry.

For the iodide complex as an example, the Ni–N(tmen) bond lengths (2.138(4) and 2.155(4) Å and Ni–O(bzac) 2.005(3) and 2.036(3) Å) are similar to those of [$Ni_2(CO_3)$-$(acac)_2(tmen)_2$]: Ni–N 2.156(3), 2.123(3) and Ni–O 2.018(3), 2.004(3) Å.[9] Two aqua ligands are in a cis-geometry, similar to the aqua ligand and the methanol in [Ni(acac)(tmen)-(H_2O)(CH_3OH)]ClO_4.[10] The Ni–O(H_2O) bond lengths of 2.086(4) and 2.119(3) Å are not very different from the Ni–

$O(CH_3OH)$ bond length of 2.094(3) Å and that of the Ni–$O(H_2O)$ bond, 2.160(3) Å, of $[Ni(acac)(tmen)(H_2O)(CH_3OH)]ClO_4$. The difference in the bond length Ni–$O(H_2O)$ in the complexes **2** and **3** shows that in those complexes, one of the water molecules more loosely coordinates to the metal than the other. A slight distortion of the octahedron is evident from the angles around nickel: the five-membered chelate ring, i.e. N(1)–Ni–N(2) (Ni-tmen), observed as 84.6(2)° is smaller than that of the six-membered ring O(1)–Ni–O(2) (Ni-bzac) of 89.6(1)°, which is in good agreement with those of $[Ni_2(ox)(acac)_2(tmen)_2]\cdot 2TCE$ (TCE = 1,1,2,2-tetrachloroethane): N(1)–Ni–N(2) (Ni-tmen) and O(1)–Ni–O(2) (Ni-acac) of 84.4(2)° and 89.9(2)°, respectively.[10]

The chloride complex has a similar configuration where the chloro ligand and the aqua ligand are again in a cis-position; the Ni–O(bzac) bond lengths, 2.032(3) and 2.015(3) Å, and the bite angle, O(1)–Ni(1)–O(2) of 90.9(1)°, of bzac are similar to those of the iodide. However, the Ni–N(tmen) bond lengths, 2.195(4) and 2.191(5) Å, are slightly longer than those of the iodide, 2.138(4) and 2.155(4) Å, and the tmen bite angle, N(1)–Ni(1)–N(2), of 83.5(2)° is smaller than that of the iodide case, i.e. 84.6(2)°. This smaller bite angle gives the chloride complex a more distorted octahedral environment than the iodide or bromide complex.

Selected non-bonded contacts for all of the complexes are given in Table 2. Figure 2 illustrates the H-bonded dimerization in the chloride complex **1**, and the ladder-like hydrogen bond network formed in the bromide and iodide complexes **2** and **3**. In the complexes (**2** and **3**), two layers of halide complexes (each layer is represented by only one molecule in the

Table 2. Non-Bonded Contacts for $Ni(tmen)(bzac)X\cdot n(H_2O)$ (X = Cl, Br, and I, n = 1–4)

Non-bonded contacts out to 3.60 Å for $[NiCl(bzac)(tmen)(H_2O)]$					
Cl(1)–O(3)[a)]	3.160(4)	O(1)–O(3)[a)]	2.861(5)	O(3)–O(3)[a)]	3.219(8)
O(3)–C(10)[b)]	3.507(8)	O(3)–Cl(5)[a)]	3.551(6)	C(9)–C(15)[c)]	3.578(9)
C(16)–C(16)[d)]	3.31(1)				
Non-bonded contacts out to 3.60 Å for $[Ni(bzac)(tmen)(H_2O)_2]Br\cdot 2H_2O$					
Br(1)–O(6)[e)]	3.326(4)	Br(1)–O(5)	3.334(3)	Br(1)–O(4)[f)]	3.407(3)
Br(1)–O(3)[e)]	3.368(3)	O(2)–O(5)	2.741(4)	O(4)–O(5)	2.845(5)
O(3)–O(6)[g)]	2.696(5)	O(5)–O(6)	2.771(5)	O(5)–C(14)[f)]	3.448(6)
Non-bonded contacts out to 3.74 Å for $[Ni(bzac)(tmen)(H_2O)_2]I\cdot 2H_2O$					
I(1)–O(5)[h)]	3.524(4)	I(1)–O(6)[i)]	3.526(4)	I(1)–O(3)	3.596(4)
I(1)–O(4)[i)]	3.653(4)	O(2)–O(5)[i)]	2.731(4)	O(3)–O(6)	2.720(6)
O(4)–O(5)[i)]	2.791(6)	O(5)–O(6)	2.796(6)	O(5)–C(14)	3.530(7)

Symmetry operations: a) $-x+2, -y, -z+2$. b) $x, y-1, z$. c) $-x+1, -y+1, -z+2$. d) $-x+1, -y, -z+2$. e) $x, -y-1/2, z+1/2$. f) $-x+1, y-1/2, -z+1/2$. g) $-x+1, -y, -z$. h) $-x+2, y-1/2, -z-1/2$. i) $x+2, -y, -z$.

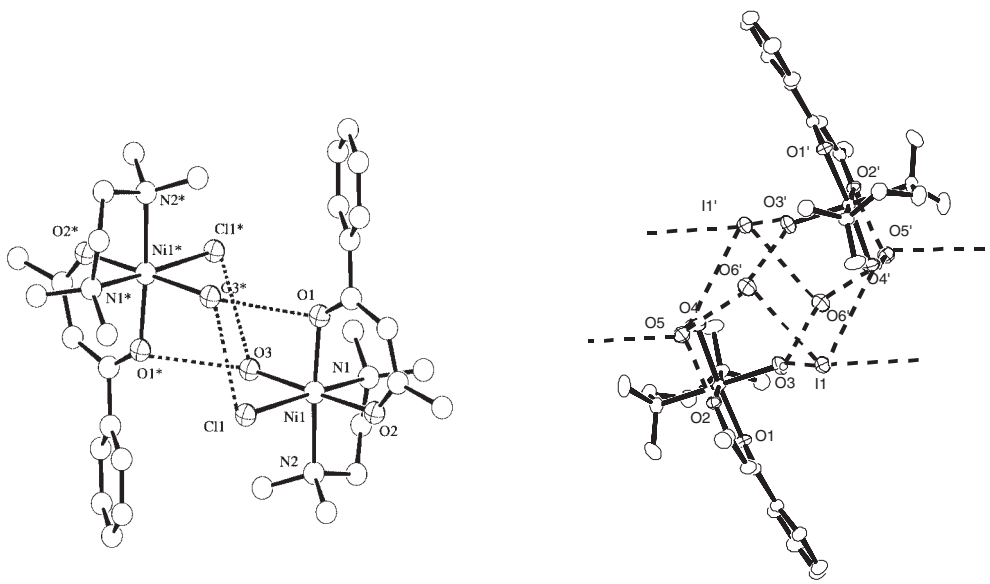

Fig. 2. ORTEP drawings of two dimerically hydrogen bonded $[NiCl(bzac)(tmen)(H_2O)]$ molecules (left) and hydrogen bond network formed in $[Ni(bzac)(tmen)(H_2O)_2]I\cdot 2H_2O$ (right). Hydrogen atoms are omitted for clarity. Displacement ellipsoids are drawn at 30% probability. The primed or asterisked atoms are related to the unique set by a center of symmetry, i.e. −x, −y, −z.

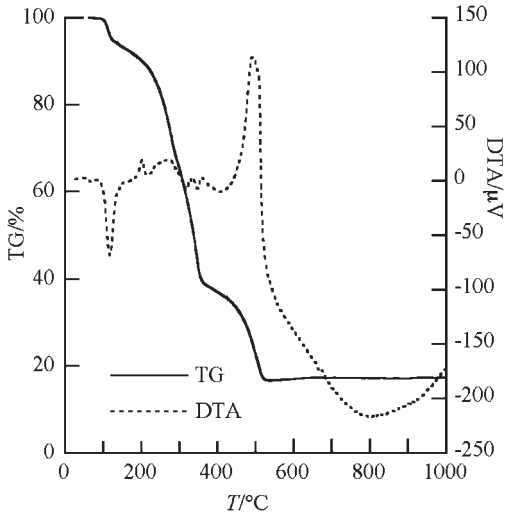

Fig. 3. Thermal analysis of [NiCl(bzac)(tmen)(H_2O)].

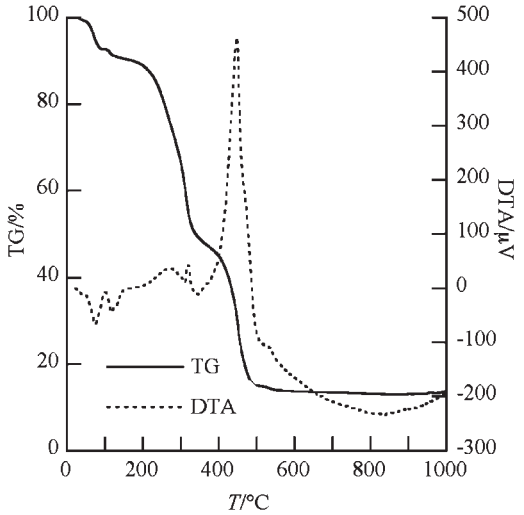

Fig. 5. Thermal analysis of [Ni(bzac)(tmen)(H_2O)$_2$]I·2H_2O.

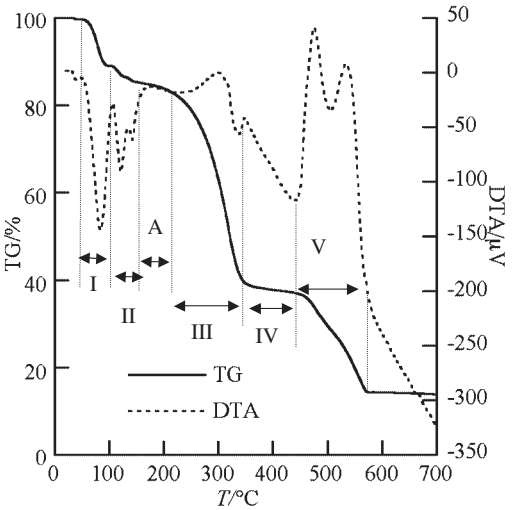

Fig. 4. Thermal analysis of [Ni(bzac)(tmen)(H_2O)$_2$]Br·2H_2O. 3H_2O are lost in phase I, one H_2O is lost in phase II, disproportionation yields a mixture of [$NiBr_2$(tmen)] and [Ni(bzac)$_2$(tmen)] in phase A, tmen is released in phase III, $NiBr_2$ is maintained in phase IV, bzac moiety is released and $NiBr_2$ is decomposed oxidatively in phase V to yield NiO.

figure) are separated by a sort-of-inorganic channel comprising water of crystallization and halide anions, while in complex **1**, two neighboring molecules are tightly bonded by strong H bonds to form a dimer.

Thermochemical Reactions of the Halide Complexes in the Solid State. The results of a TG-DTA analysis of three complexes are shown in Figs. 3, 4, and 5. The weight losses observed in the TG curves of bromide **2** and iodide **3** before 100 °C and the corresponding endothermic DTA peaks are due to the liberation of the water of crystallization. This is consistent with the previously reported results of bis-diamine complexes of Ni(II).[11,12] The chloride complex (**1**), on the other hand, loses one coordinated water molecule between ca. 90 and ca. 130 °C. Complex **1** then shows three big weight losses, which occur in 5 steps, as suggested by the corresponding DTA peaks, particularly the last one with a big exotherm (probably combustion). As the residue, we obtained NiO (mass loss found, 83.2%; calculated, 81.7%). In the case of the iodide complex, the close examination of the DTA peak predicts that the afore-mentioned removal of crystallization water actually occurs in two steps. This dehydration process is followed by the elimination of one coordinated water (presumably it must be the one that coordinates more loosely to the Ni(II)). Complex **3** then undergoes three big mass losses. In particular, the last weight loss is also accompanied by a prominent exotherm. The residue was NiO (mass loss found, 86.8%; calculated, 86.1%).

Detailed Thermal Reaction and Possible Reaction Mechanism. The bromide complex **2** loses 3 water molecules in one step, as is evident from the TG and DTA curves (shown as phase I in Fig. 4). This means that two water molecules of crystallization and one coordinated water are removed at the same time. We repeated the measurement at a slower heating rate of 2 °C/min, but obtained an identical result. The last water molecule is released from complex **2** between ca. 90 and ca. 170 °C (phase II), apparently in two steps. Then, complex **2** again undergoes three major weight losses, but different from complexes **1** and **3**; here, the last two major losses occur continuously. The residue was NiO (mass loss found, 86.85%; calculated, 84.7%). In order to observe the thermal color change of the bromide complex, complex **2** was heated at 120 °C under a vacuum in a transparent glass tube. The original pale blue–green color of [Ni(bzac)(tmen)(H_2O)$_2$]Br·2H_2O turned to yellowish green after 20 hours, dark brown after 50 hours, and finally the compound became a black/purple resinous solid (after 74 hours). The IR spectrum of the yellowish-green product was very similar to that of the starting material, suggesting that a major structural change did not occur at this stage. The black/purple material was very hygroscopic, which did not allow us to conduct an IR measurement employing KBr; however, the spectrum taken with Nujol-mull revealed that this material contained bzac and tmen moieties, but did not contain any water. Therefore, the chemical formula of this material shall be expressed as Ni(tmen)(bzac)Br. The black/

Table 3. Mass Spectra of [$NiBr_2$(tmen)], [Ni(bzac)$_2$(tmen)], and Black/Purple Substance

	m/z
[$NiBr_2$(tmen)]	58(Ni^+, 100%), 116($tmen^+$, 8%), 253(Ni(tmen)^{79}Br, 20%), 255(Ni(tmen)^{81}Br, 28%), 332(Ni(tmen)$^{79}Br_2$, 3%), 334(Ni(tmen)^{79}Br^{81}Br, 6%), 336(Ni(tmen)$^{81}Br_2$, 5%)
[Ni(bzac)$_2$(tmen)]	58(Ni^+, 100%), 77(phenyl$^+$, 39%), 105(benzoyl$^+$, 80%), 161($bzac^+$, 30%), 162($bzacH^+$, 42%), 219(Ni(bzac), 27%), 220(Ni(bzacH), 68%), 365(Ni(bzac)$_2$–methyl, 43%), 380(Ni(bzac)$_2$, 100%), 382(Ni(bzacH)$_2$, 67%)
Black/purple substance	58(Ni^+, 100%), 77(phenyl$^+$, 28%), 105(benzoyl$^+$, 61%), 116($tmen^+$, 20%), 161($bzac^+$, 18%), 162($bzacH^+$, 18%), 219(Ni(bzac), 20%), 220(Ni(bzacH), 55%), 253(Ni(tmen)^{79}Br, 73%), 255(Ni(tmen)^{81}Br, 98%), 365(Ni(bzac)$_2$–methyl, 35%), 380(Ni(bzac)$_2$, 100%), 382(Ni(bzacH)$_2$, 55%)

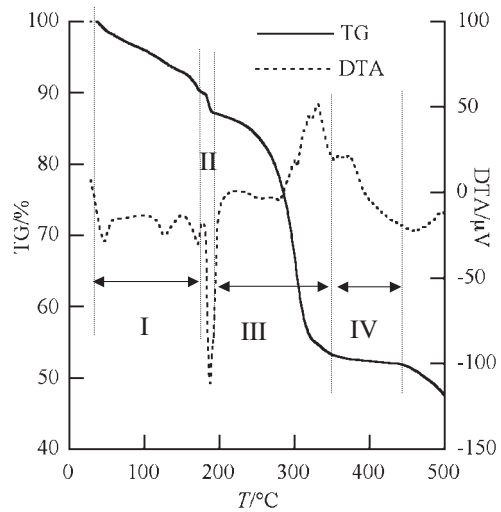

Fig. 6. Thermal analysis of [$NiBr_2$(tmen)(H_2O)$_2$]. 2H_2O are lost in phase I. HBr is released in phase II, tmen is eliminated in phase III.

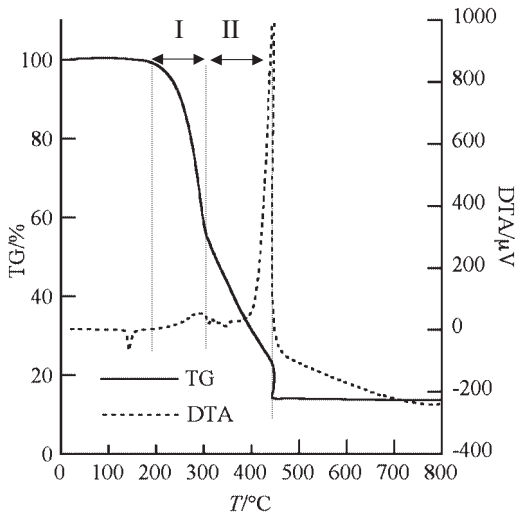

Fig. 7. Thermal analysis of [Ni(bzac)$_2$(tmen)]. Tmen is released in phase I, bzac moiety is oxidatively lost in phase II.

purple color suggested that this material was a mixture of disproportionation products, i.e. [$NiBr_2$(tmen)] (purple) and [Ni(bzac)$_2$(tmen)] (blue). We synthesized [$NiBr_2$(tmen)][13] and [Ni(bzac)$_2$(tmen)],[14] and compared their respective mass spectrum. Table 3 lists the peaks of the black/purple substance given together with those of the disproportionation products. Superimposition of the spectrum of [$NiBr_2$(tmen)] and that of [Ni(bzac)$_2$(tmen)] resulted in the spectrum of the black/purple substance, supporting the presumption that this was a mixture of these disproportionation products. Coming back to the TG/DTA chart of the bromide complex, we can now propose a hypothetical idea that complex **2** undergoes disproportionation during the relatively flat period (shown as phase A in Fig. 4) after dehydration and before a big drop in the mass, yielding [$NiBr_2$(tmen)] and [Ni(bzac)$_2$(tmen)] at around 150 °C. What attracted our attention was that both of the disproportionation products were present at this stage as a mixture, and that the nickel(II) bis-diketonato complex that we obtained was nonvolatile, in contrast to the results of the previous work.[7]

Now that we had confirmed the substance existing in phase A is a mixture of two disproportionation products, analyses of the phase III, phase IV, and phase V were carried out by comparing Fig. 4 with the TG/DTA curves obtained on [$NiBr_2$(tmen)] and [Ni(bzac)$_2$(tmen)].

Figures 6 and 7 show the results of the TG-DTA analysis of [$NiBr_2$(tmen)(H_2O)$_2$] and [Ni(bzac)$_2$(tmen)] respectively. [$NiBr_2$(tmen)(H_2O)$_2$] loses the two coordinated water between ca. 35 °C and ca. 180 °C (phase I) to become [$NiBr_2$(tmen)], loses 3.1% of the initial weight during an eminent endothermic reaction (phase II)[16] then loses 31.3% of the initial weight (which corresponds to a molecular mass of 116 = tmen) in phase III, turning into $NiBr_2$ which is apparently stable up to ca. 440 °C (phase IV). The phase III and the phase IV in Fig. 4 bear a striking resemblance to the phase III and the phase IV of Fig. 6; we can therefore presume that [$NiBr_2$(tmen)] produced in phase A releases tmen in phase III, yielding $NiBr_2$, which is stable during phase IV, and then undergoes an oxidation process in phase V, yielding the final product, NiO.

The other species co-existing in phase A, [Ni(bzac)$_2$(tmen)], melted at around 140 °C, as shown in Fig. 7, then a total of 85.8% of weight loss was observed with two exotherms, around 300 °C and around 450 °C, respectively; the residue was NiO (mass loss found, 85.8%; calculated, 85.0%). It is most likely that here again the complex lost tmen in the first

exothermic process, since firstly the corresponding DTA peaks were of the same order; secondly, the release of tmen took place at around 300 °C; thirdly, since tmen is a molecular substance and bzac is an ionic ligand, tmen more easily dissociates from the central metal than bzac. Therefore, we presume that $[Ni(bzac)_2(tmen)]$ releases tmen in phase I, followed by elimination of the bzac moiety in phase II, leaving NiO as the final product. A comparison between Fig. 4 and Fig. 7, gives us an assumption that $[Ni(bzac)_2(tmen)]$ produced in phase A releases tmen in phase III, and then the bzac moiety undergoes an oxidation process in phase V, yielding the final product, NiO. The assumed thermal reaction and reaction mechanism are summarized in the scheme given in Fig. 8.

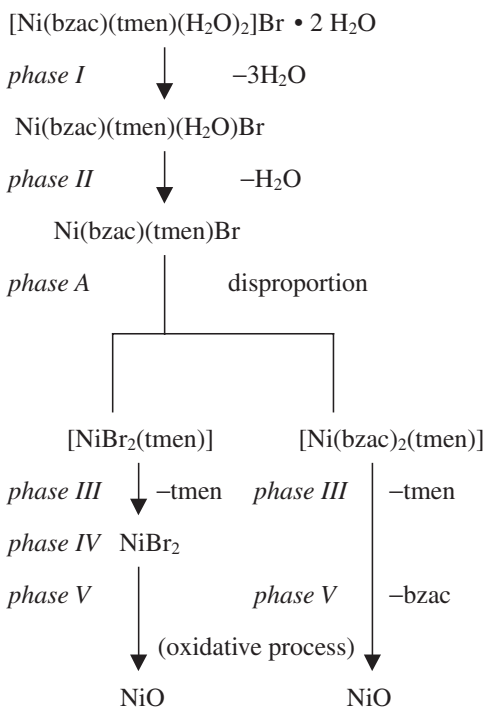

Fig. 8. Assumed thermal reaction and reaction mechanism of $[Ni(bzac)(tmen)(H_2O)_2]Br \cdot 2H_2O$.

Fig. 9. $[Ni(bzac)(tmen)(H_2O)_2]I \cdot 2H_2O$ in 4 different organic solvents, namely nitromethane (NM), 1,2-dichloroethane (DCE), acetone (ACO), and dimethylsulfoxide (DMSO) (from the left).

Spectral Behavior of Complexes 1–3 in Various Organic Solvents. All of these three complexes showed significant solvatochromism. The original green color of complex **3** is changed when dissolved in various organic solvents (see Fig. 9). The electronic spectra of $[NiCl(bzac)(tmen)(H_2O)]$, $[Ni(bzac)(tmen)(H_2O)_2]Br \cdot 2H_2O$, and $[Ni(bzac)(tmen)(H_2O)_2]I \cdot 2H_2O$ in various organic solvents with different donor/acceptor abilities were measured, and are shown in Figs. 10–12, with their ν_{max} values summarized in Table 4.

Dimethylsulfoxide (DMSO): The spectral patterns of complexes **1**, **2**, and **3** in DMSO are very similar, since each complex has two absorption peaks (ν_1 and ν_2 transitions 9.43, 15.90 (**1**), 9.41, 15.90 (**2**), and 9.40, 15.92 (**3**) (unit: $\times 10^3$ cm^{-1}) are assigned as $^3A_{2g} \rightarrow {}^3T_{2g}$, $^3A_{2g} \rightarrow {}^3T_{1g}$, respectively), indicating that these mixed-ligand complexes form 6-coordinate species in DMSO. The electric molar conductances of the solutions ranging between 22.36 and 28.77 [Standard

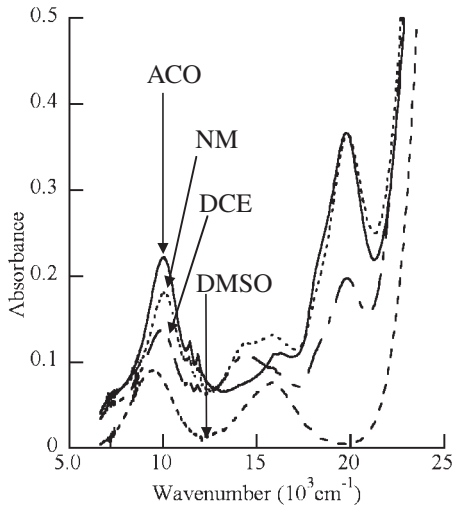

Fig. 10. Electronic spectra of complex **1** in various solvents (concentration: 1.00×10^{-2} mol dm^{-3}, measured at room temperature).

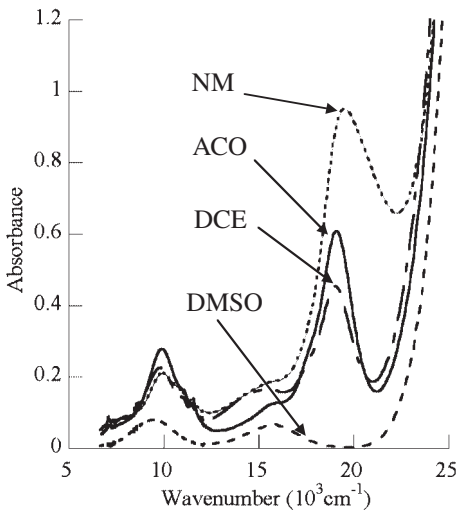

Fig. 11. Electronic spectra of complex **2** in various solvents (concentration: 1.00×10^{-2} mol dm^{-3}, measured at room temperature).

Table 4. Spectral Data of Solutions of the Halide Complexes **1**, **2**, and **3** in Various Organic Solvents $\nu_{max}/10^3$ cm^{-1}

Solvent	Complex	ν_{max}					
	1	9.43	15.90				
DMSO	**2**	9.41	15.90				
	3	9.40	15.92				
	1	10.09	11.37	11.81	15.90	19.84	
NM	**2**	9.92	11.05 (sh)	11.53	15.97	19.53	
	3						20.59
	1	9.93	11.41	11.87	14.43	19.80	
DCE	**2**	9.81	11.06 (sh)	11.52	15.43	19.02	
	3	9.64			14.5 (sh)	17.60	22.07
	1	10.05	11.42	11.86	16.29	19.73	
ACO	**2**	9.89	11.03 (sh)	11.53	15.78	19.05	
	3	9.54			14.5 (sh)	17.71	22.11

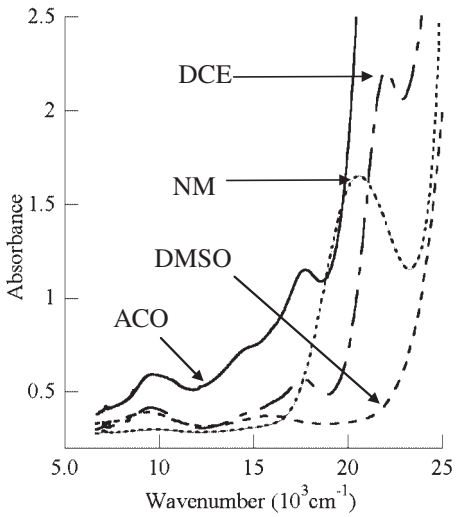

Fig. 12. Electronic spectra of complex **3** in various solvents (concentration: 1.00×10^{-2} mol dm^{-3}, measured at room temperature).

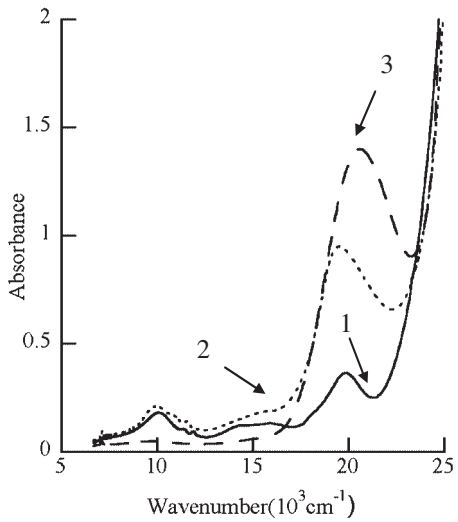

Fig. 13. Electronic spectra of complexes **1**, **2**, and **3** in NM.

value of the 1:1 electrolyte solution = ca. 32 (Λ_M/S cm^2 mol^{-1})][17] show that the halide anions exist as free anions, i.e. do not coordinate to nickel cations. Therefore, the species present in this highly polar and strong coordinating solvent can be most probably expressed as [Ni(bzac)(tmen)(dmso)$_2$]$^+$ and X$^-$, because the aqua ligands are naturally replaced by the strong coordinating solvent molecules, and these spectra are similar to the corresponding [Ni(bzac)(tmen)](BPh$_4$) in the solvent.[15]

Nitromethane (NM): The spectral behaviors of the complexes in nitromethane are different among the complexes (Fig. 13). The fact that the iodide complex **3** has only one absorption peak at 20.6×10^3 cm^{-1} (assigned as $^1A_{1g} \rightarrow {}^1B_{1g}$) suggests that complex **3** has a square–planar geometry in nitromethane. Showing the same spectra as that of [Ni(bzac)(tmen)](BPh$_4$) in this solvent (20.4×10^3 cm^{-1}),[15] this also proves complex **3**, just like [Ni(acac)(tmen)(H$_2$O)$_2$](ClO$_4$), releases two water molecules when dissolved in nitromethane, and exists as a cation having a square–planar geometry.[15,18] Since nitromethane is a medium-level acceptor and a very weak donor solvent, the positively charged Sp species is stabilized in solution.

In the spectra of chloride and bromide complexes (**1** and **2**), four more peaks including shoulders were observed in addition to a big absorption peak around 19×10^3 cm^{-1}, suggesting the occurrence of a disproportionation reaction. Besides, the absorption peak of complex **2** at 19.53×10^3 cm^{-1} is somewhat tilted to the left, suggesting the presence of the Sp species having a ν_{max} value of around 20.4×10^3 cm^{-1}; we measured the absorption spectra of [NiBr$_2$(tmen)](Td), [Ni(bzac)$_2$(tmen)](Oh), and [Ni(bzac)(tmen)](BPh$_4$)(Sp) and compared them with that of complex **2** (Fig. 14). It is clearly shown that the solid line obtained by adding the spectra of Td, Oh, and Sp species overlaps the spectrum of complex **2** very well. This means that complex **2** undergoes both deaquation (yielding Sp) and disproportionation (yielding Td and Oh). On the other hand, complex **1** in the solvent has a peak at 19.84×10^3 cm^{-1}, which has a symmetric form, and is free from any sign of the Sp species; we conclude that the chloride complex undergoes only disproportionation.

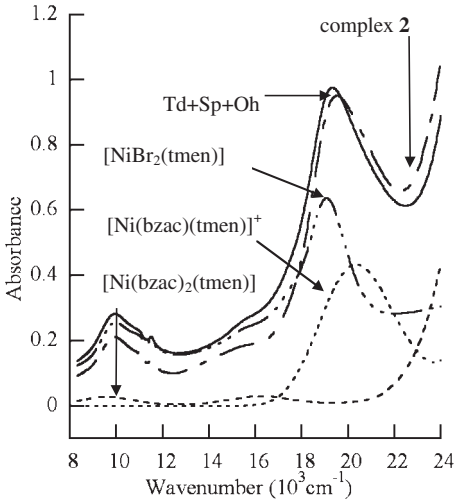

Fig. 14. Composition of the spectra of $[NiBr_2(tmen)]$ (Td species), $[Ni(bzac)(tmen)]^+$ (Sp species), $[Ni(bzac)_2$-(tmen)] (Oh species), and complex **2** in NM.

1,2-Dichloroethane (DCE): The spectral patterns of complexes **1**, **2**, and **3** in DCE (see Figs. 10–12) suggest that these complexes undergo a disproportionation reaction again in DCE and yield the Td and Oh species. As it is clear from Fig. 14, the absorption of the Oh species is negligible compared to that of the Td species; we can presume that these ν_{max} values are attributable mainly to the Td species. On this basis, the bands at 9.93, 9.81, and 9.64 (unit: $\times 10^3$ cm^{-1}) are assigned to ν_2 $^3T_1(F) \rightarrow {}^3A_2(F)$, and the bands at 19.80, 19.02, and 17.60 (unit: $\times 10^3$ cm^{-1}) as ν_3 $^3T_1(F) \rightarrow {}^3T_1(P)$. (The bands to be assigned to ν_1 transition $^3T_1(F) \rightarrow {}^3T_2(F)$ were not observed.) The two peaks (or a shoulder) at 11.06–11.87 (unit: $\times 10^3$ cm^{-1}) observed with complexes **1** and **2** are assigned to a spin-forbidden transition to an upper state arising from the ^1D state of the free ion.[19] The band observed with complex **3** at 22.07×10^3 cm^{-1} can be assigned to a charge-transfer transition. What is left is the bands observed with three complexes at 14.43, 15.43, and 14.5(sh) (unit: $\times 10^3$ cm^{-1}), respectively. In order to investigate the origin of this band, we measured the time-course change in the absorbance of complex **2** dissolved in DCE. The result is shown in Fig. 15. It is clear from the chart that the amount of the Td species (which is indicated by the absorption at ν_{max} of 9.81, 11.06(sh), 11.52, and 19.02×10^3 cm^{-1}) increases with time, while an unknown species having the absorption at 14.73×10^3 cm^{-1} decreases. This suggests that complex **2** in DCE undergoes disproportionation via an intermediate compound having a ν_{max} of around 15×10^3 cm^{-1}. L. Sacconi has reported that a five-coordinate Nickel(II) containing tris(2-dimethylaminoethyl)amine and a bromide anion has an absorption peak at 14.5×10^3 cm^{-1}.[1] These data suggest that the above-mentioned intermediate of this disproportionation reaction having a ν_{max} of 14.73×10^3 cm^{-1} is also a 5-coordinate species. Assuming that [NiBr(bzac)(tmen)] (5-coordinate) can be produced by a reaction between [Ni(bzac)-(tmen)](BPh_4) and tetrabutylammonium bromide, we mixed equimolar amounts of [Ni(bzac)(tmen)](BPh_4) and tetrabutylammonium bromide in DCE and measured the time-course change of the spectrum of the resulting solution. Figure 16 shows exactly the same change in the spectral pattern as we

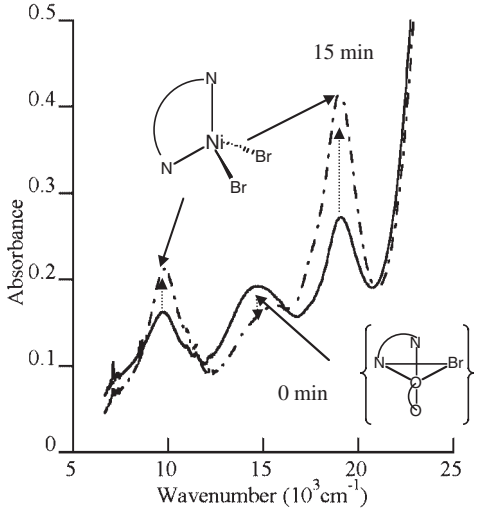

Fig. 15. Time-course change in the absorbance of [Ni-(bzac)(tmen)$(H_2O)_2$]Br$\cdot 2H_2O$ dissolved in DCE.

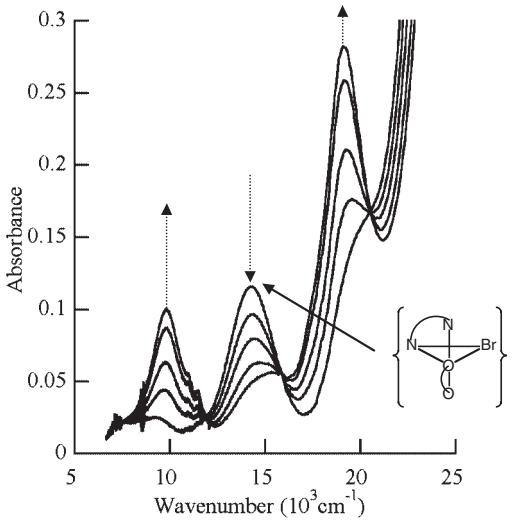

Fig. 16. Time-course change in absorbance of DCE in which [Ni(bzac)(tmen)](BPh_4) and tetrabutylammonium bromide were mixed.

obtained with complex **2**. Therefore, it may be reasonable to conclude that complex **2** undergoes disproportionation in DCE via a 5-coordinated intermediate complex:

$$[Ni(bzac)(tmen)(H_2O)_2]Br\cdot 2H_2O \rightarrow [NiBr(bzac)(tmen)] + 4H_2O \rightarrow 1/2[Ni(bzac)_2(tmen)] + 1/2[NiBr_2(tmen)]. \quad (1)$$

Acetone (ACO): The spectra of complexes **1**, **2**, and **3** in ACO are conformal to those in DCE, and we could ultimately obtain exactly the same spectral change as those obtained in DCE when we mixed equimolar amounts of [Ni(bzac)(tmen)]-(BPh_4) and tetrabutylammonium bromide in ACO. Therefore, we can conclude that three complexes undergo disproportionation in acetone as well.

Conclusion

$Ni(tmen)(bzac)X\cdot n(H_2O)$($n = 1$ for X = Cl, and $n = 4$ for X = Br or I) undergo deaquation and disproportionation both

in various organic solvents and in the solid state. Their behavior in solution depends on the coordination ability of the anions (X^-), and the nature of the solvents, more specifically, on the acceptor and/or donor properties of the solvents.

1) In a strong donor solvent such as DMSO, all of complexes **1**, **2**, and **3** are subject to deaquation, followed by solvent coordination, yielding the Oh species:

$$\mathrm{Ni(tmen)(bzac)X\cdot}n\mathrm{(H_2O)} + 2\ \text{solvent} \rightarrow [\mathrm{Ni(bzac)(tmen)(solvent)_2}]^+ + \mathrm{X}^- + n\mathrm{H_2O}. \quad (2)$$

The resulting Oh species is stable, as Ni(II) with the d^8 configuration preferring the Oh configuration from the view point of the structural preference energies;[20] the complex cation is solvated and stabilized by DMSO having a large donor number (DN = 29.8). In addition to that, the relatively large acceptor capacity of DMSO also stabilizes the resulting halide anion, X^-.

2) In a medium-level acceptor and a very weak donor solvent, such as NM, complex **1** undergoes only a disproportionation reaction, yielding the Td and Oh species; complex **2** undergoes both deaquation and disproportionation, yielding the Sp, Td, and Oh species; and complex **3** undergoes only deaquation, yielding the Sp species:

$$\mathrm{Ni(tmen)(bzac)X\cdot}n\mathrm{(H_2O)} \rightarrow [\mathrm{Ni(bzac)(tmen)}]^+ + \mathrm{X}^- + n\mathrm{H_2O}, \quad (3)$$

$$2\{\mathrm{Ni(tmen)(bzac)X\cdot}n\mathrm{(H_2O)}\} \rightarrow [\mathrm{Ni(bzac)_2(tmen)}] + [\mathrm{NiX_2(tmen)}] + 2n\mathrm{H_2O}. \quad (4)$$

If tmen and bzac are regarded as being strong ligands, then the Ni(II) ions prefer a low-spin state and the Sp configuration, and only deaquation will take place. This is the case of iodide, which is bulky and has a weak coordination power. However, since the chloride anion has a higher ligand field strength and smaller size, the resulting Td species, i.e. $[NiCl_2(tmen)]$, is more stable; in addition to this, the by-produced tris chelate product, $[Ni(bzac)_2(tmen)]$, is very stable due to its Oh configuration and chelating effect; the $[Ni(bzac)(tmen)]^+$ and X^- will further undergo a disproportionation reaction. The bromide ion, having an intermediate coordination capacity and size, follow both reaction schemes (Equations 3 and 4).

3) In rather inert solvents with weak acceptor and weak donor properties, such as DCE and ACO, all complexes, **1**, **2**, and **3** undergo the disproportionation reaction. The donor and acceptor properties of these solvents are not strong enough to solvate and stabilize the ionic species, i.e. the positively charged complex ions and the negatively charged halide anions. The presence of a proposed intermediate (5-coordinate compound) suggests that the halide anion is coordinated to the Ni(II) after deaquation, and then disproportionation takes place.

When compared to the former study carried out by Hoshino et al.,[6] the largest difference found between the Ni(tmen)(acac)X and Ni(tmen)(bzac)X (X = halide) systems is that during the thermal reaction, the $[Ni(bzac)_2(tmen)]$ does not evaporate following the disproportionation, thereby providing a mixture of dihalo and bis(benzoylacetonato) complexes. As we expected, a nonvolatile bis-β-diketonate ternary complex was synthesized by the use of the β-diketone having an aromatic substituent. $Ni(tmen)(acac)_2$ is very soluble in a nonpolar solvent, such as hexane.[7] The solubility of $[Ni(bzac)_2(tmen)]$ in nonpolar solvents is lower than that of $[Ni(acac)_2(tmen)]$, which suggests that the bis-bzac ternary complex has a higher molecular interaction than that of the bis-acac analogue; therefore, the volatility is decreased.

Experimental

Instrumentation. Electronic spectra between 400 nm and 1200 nm of the solutions were obtained on a Shimadzu UV-3100PC UV–vis Scanning Spectrophotometer using 10 mm quarts cells at a concentration of 1.0×10^{-2} mol dm^{-3}. IR spectra between 330 and 5000 cm^{-1} were measured on a Perkin-Elmer FT-IR SPECTRUM 2000 using the KBr method and Nujol-mull. Electric conductances of the solutions (concentrations of 1.0×10^{-3} M) were measured with a TOA Conductivity Outfit Model CM 40-G at 25 ± 0.1 °C. Elemental analyses were performed on a Perkin-Elmer 2400II CHN analyzer. Thermal analyses (TG and DTA) were carried out using a Shimadzu "Stand Alone" thermal analyzer (TGA-50H, DTA-50) and the associated data acquisition and handling system, TA-50 WSI, in static air up to 1000 °C, at a heating rate of 10 °C/min, unless otherwise stated. A sample of ca. 7 mg was placed in an uncovered alumina cell, and highly sintered α-Al_2O_3 (Shimadzu) was employed as a DTA reference material. Mass spectra (EI, 70 eV) were taken on a JEOL JMS-700 MStation. All of the measurements were carried out at room temperature, unless otherwise specified.

Materials. All materials used were purchased from Wako Pure Chemical Industries Ltd. of reagent grade (extra pure) or spectroscopic grade, and were used without further purification.

Synthesis of [NiCl(bzac)(tmen)(H_2O)] (1). To a transparent yellow–green solution of 10 mmoles of $NiCl_2\cdot 6H_2O$ in 30 mL of ethanol, was added 15 mmoles of tmen dropwise with vigorously stirring; the solution turned into a green suspension. Upon the addition of 10 mmoles of benzoylacetone dissolved in 10 mL of hot ethanol, the solution turned bluish green. After stirring for 2 hours, a yellow–green precipitate was formed. Sodium carbonate (5 mmoles) was added thereto and stirred for 30 minutes; then, a blue–green clear solution containing a white precipitate was obtained. After the suspension was filtered and concentrated, the obtained solid was recrystalized from DCE in a freezer to give **1** as a green powder. Yield: 47.1%. Anal. Found: C, 49.46; H, 7.32; N, 7.31%. Calcd for $C_{16}H_{27}ClN_2NiO_3$: C, 49.40; H, 7.20; N, 6.94%. Monocrystal was obtained from ethanolic solution of the compound by slow evaporation at room temperature. IR (KBr): ν (O–H) 3370, δ (O–H) 1655, ν (C=C) 1598, ν (C=O) 1519 cm^{-1}.

Synthesis of [Ni(bzac)(tmen)(H_2O)$_2$]Br·2H_2O (2). The procedure described for synthesis of **1** was repeated, except that $NiBr_2$ and triethylamine were employed instead of $NiCl_2\cdot 6H_2O$ and sodium carbonate, respectively. Blue–green single crystals of **2** were obtained by recrystallization from ethanol at room temperature. Yield: 50.0%. Anal. Found: C, 39.11; H, 6.71; N, 5.63%. Calcd for $C_{16}H_{33}BrN_2NiO_6$: C, 39.30; H, 6.80; N, 5.73%. IR (KBr): ν (O–H) 3370, δ (O–H) 1656, ν (C=C) 1599, ν (C=O) 1518 cm^{-1}.

Synthesis of [Ni(bzac)(tmen)(H_2O)$_2$]I·2H_2O (3). The procedure described for the synthesis of **1** was repeated, except that NiI_2 was employed as the starting material and [Ni(bzac)(tmen)-(H_2O)$_2$]I·2H_2O was obtained as a green single crystal by recrystallization from ethanol. Yield: 19.8%. Anal. Found: C, 33.76; H, 5.68; N, 4.86%. Calcd for $C_{16}H_{33}IN_2NiO_6$: C, 35.90; H, 6.21; N,

Table 5. Crystallographic Data

	[NiCl(bzac)(tmen)(H_2O)]	[Ni(bzac)(tmen)(H_2O)$_2$]Br·2H_2O	[Ni(bzac)(tmen)(H_2O)$_2$]I·2H_2O
Formula	$C_{16}H_{27}ClN_2NiO_3$	$C_{16}H_{33}BrN_2NiO_6$	$C_{16}H_{33}IN_2NiO_6$
M	389.55	485.03	535.05
Crystal system	triclinic	monoclinic	monoclinic
Space group	$P\bar{1}$ (no. 2)	$P2_1/c$ (no. 14)	$P2_1/c$ (no. 14)
λ/Å	0.71069	0.71069	0.71069
a/Å	9.159(1)	14.761(1)	15.093(2)
b/Å	9.507(1)	9.9208(7)	9.925(1)
c/Å	11.849(1)	15.449(1)	15.575(2)
α/°	76.332(4)	90	90
β/°	72.599(3)	102.361(1)	102.900(4)
γ/°	79.097(4)	90	90
V/Å^3	948.8(2)	2210.0(3)	2274.2(5)
Z	2	4	4
D_{calc}/g cm^{-3}	1.363	1.458	1.563
Crystal size/mm^3	0.11 × 0.33 × 0.48	0.14 × 0.25 × 0.41	0.48 × 0.43 × 0.24
2θ Range/°	5.85–56.5	4.90–56.6	4.70–56.6
μ/cm^{-1}	11.96	27.22	22.41
Total reflections	4512	13955	14313
Unique reflections	2706	5185	5312
Observed reflections	2061[$I > 2.50\sigma(I)$]	3624[$I > 2.50\sigma(I)$]	4013[$I > 2.50\sigma(I)$]
R[a)], R_w[b)]	0.042, 0.046	0.039, 0.038	0.038, 0.038
Goodness of fit	0.17	0.05	0.07
Reflection/ Parameter Ratio	9.91	10.41	11.53

a) $R = \Sigma||F_o| - |F_c||/\Sigma|F_o|$, b) $R_w = [\Sigma(w(|F_o| - |F_c|)^2/\Sigma w|F_o|^2)]^{1/2}$ with $w = 4F_o^2/[\sigma^2(F_o^2)]$.

5.23%.[21] IR (KBr): ν (O–H) 3400, δ (O–H) 1660, ν (C=C) 1597, ν (C=O) 1520 cm^{-1}.

X-ray Crystallography. The three complexes [NiCl(bzac)(tmen)(H_2O)] (**1**), [Ni(bzac)(tmen)(H_2O)$_2$]Br·2H_2O (**2**), and [Ni(bzac)(tmen)(H_2O)$_2$]I·2H_2O (**3**) were recrystallized from ethanol–water mixtures by slow evaporation at room temperature to give transparent blue–green plates, aqua-blue blocks, and green blocks, suitable for single-crystal X-ray analysis, respectively. Crystals of complexes **1**, **2**, and **3** mounted on a glass fibers were irradiated with graphite monochromated Mo Kα radiation at 23 °C on a Bruker Smart APEX CCD diffractometer with 10, 15, and 10 sec/frame exposure times, respectively. All of the data were corrected for Lorentz and polarization effects and crystal absorption (SMART and SAINT (SADABS)).[22] However, no crystal decay corrections were necessary. The structures were solved by direct methods (SIR92)[23] and expanded using Fourier techniques (DIRDIF94).[24] The non-hydrogen atoms were refined anisotropically, while only the hydrogen atom coordinates were refined. The final cycle of full-matrix least-squares refinement[25] was based on 2061, 3624, and 4013 observed reflections and 208, 348, and 352 variable parameters and converged with unweighted agreement factors (R) equal to 0.042, 0.039, and 0.038, respectively. Neutral atom scattering factors were taken from Cromer and Waber.[26] Anomalous dispersion effects were included in F_{calc};[27] the values for Df' and Df'' were those of Creagh and McAuley.[28] The values for the mass-attenuation coefficients are those of Creagh and Hubbel.[29] All calculations were performed using the teXsan[30] crystallographic software package of Molecular Structure Corporation. Selected crystallographic data and refinement parameters are given in Table 5.

The authors thank Prof. Yoichi Ishii, Chuo University, for his help with elemental analysis, Dr. Marilena Ferbinteanu, University of Bucharest, for her help with thermal analysis, and Dr. Yukie Mori, Ochanomizu University, for her valuable discussions.

References

1 L. Sacconi, "Electronic Structure and Stereochemistry of Ni(II)," in "Transition Metal Chemistry," Marcel Dekker, Inc., New York (1968), Vol. 4.

2 R. Yamamoto and T. Maruyama, Jpn. Kokai Tokkyo Koho JP 06073169 (1994); Y. Masuda and F. Inatsugu, Jpn. Kokai Tokkyo Koho JP 50121176 (1975); M. L. Golden, J. C. Yarbrough, J. H. Reibenspies, N. Bhuvanesh, P. L. Lee, Y. Zhang, and M. Y. Darensbourg, 228th ACS National Meeting, Philladelphia, PA, United States, August 22–26 (2004); C. A. Fontan, R. A. Olsina, *Talanta*, **36**, 945 (1989).

3 K. Sone and Y. Fukuda, "Inorganic Thermochromism," in "Inorganic Chemistry Concepts," Springer, Heidelberg (1987), Vol. 10; Y. Fukuda and K. Sone, *J. Inorg. Nucl. Chem.*, **37**, 455 (1975); Y. Fukuda, R. Morishita, and K. Sone, *Bull. Chem. Soc. Jpn.*, **49**, 1017 (1976); N. T. Nga, Y. Fukuda, and K. Sone, *Bull. Chem. Soc. Jpn.*, **50**, 154 (1977).

4 W. Linert, Y. Fukuda, and A. Camard, *Coord. Chem. Rev.*, **281**, 113 (2001).

5 H. Ohtsu and K. Tanaka, *Inorg. Chem.*, **43**, 3024 (2004).

6 N. Hoshino, Y. Fukuda, and K. Sone, *Bull. Chem. Soc. Jpn.*, **54**, 420 (1981).

7 Y. Saito, T. Takeuchi, Y. Fukuda, and K. Sone, *Bull.*

Chem. Soc. Jpn., **54**, 196 (1981).

8 CCDC 236626, CCDC 236627, and CCDC 236628 contain the supplementary crystallographic data for this paper. These data can be obtained free of charge from The Cambridge Crystallographic Data Centre via www.ccdc.cam.ac.uk/data_request/cif.

9 K. Yamada, K. Hori, and Y. Fukuda, *Acta Crystallogr.*, **C49**, 445 (1993).

10 K. Yamada, Y. Fukuda, T. Kawamoto, Y. Kushi, W. Mori, and K. Unoura, *Bull. Chem. Soc. Jpn.*, **66**, 2758 (1993).

11 D. M. L. Goodgame and L. M. Venanzi, *J. Chem. Soc.*, **1963**, 616.

12 R. Tsuchiya, S. Joba, A. Uehara, and E. Kyuno, *Bull. Chem. Soc. Jpn.*, **46**, 1454 (1973).

13 $[NiBr_2(tmen)]$ was obtained as a purple microcrystalline powder by dehydrating a green powder of $[NiBr_2(tmen)(H_2O)_2]$ in vacuum at 120 °C for 3 days; $[NiBr_2(tmen)(H_2O)_2]$ was synthesized from an ethanolic solution of $[NiBr_2]$ by addition of tmen; Anal. Found: C, 19.98; H, 5.42; N, 7.61%. Calcd for $C_6H_{20}Br_2N_2NiO_2$: C, 19.44; H, 5.44; N, 7.56%.

14 $[Ni(bzac)_2(tmen)]$ was synthesized in a process analogous to that reported;[15] Anal. Found: C, 62.02; H, 6.86; N, 5.58%. Calcd for $C_{26}H_{34}N_2NiO_4$: C, 62.80; H, 6.89; N, 5.63%.

15 Y. Fukuda and K. Sone, *J. Inorg. Nucl. Chem.*, **34**, 2315 (1972).

16 The green powder of $Ni(tmen)(H_2O)_2Br_2$ on heating yields purple microcrystals of $Ni(tmen)Br_2$ mixed with a small amount of a pale green substance. This pale green substance could not be eliminated even by prolonged heating. We now assume that this green substance is a trimer of $Ni(tmen)Br_2$ which is formed according to the formula;

$$3\ Ni(tmen)Br_2 + H_2O \rightarrow Ni_3(tmen)_3Br_5(OH) + HBr.$$

We have observed this trimer formation of $Ni(tmen)Br_2$ in various organic solvents and this will be reported elsewhere.

17 W. J. Geary, *Coord. Chem. Rev.*, **7**, 81 (1971).

18 A. B. P. Lever, "Inorganic Electronic Spectroscopy," Elsevier, Amsterdam (1984).

19 L. Sacconi, I. Bertini, and F. Mani, *Inorg. Chem.*, **6**, 262 (1967).

20 K. F. Purcell and J. C. Kotz, "Inorganic Chemistry," W. B. Saunders Company, Hong Kong (1977).

21 The difference between the calculated value and the observed value may be attributed to absorption of water. During the storage, we observed that once-transparent mono crystal turned opaque.

22 SMART and SAINT, Siemans (1995), Siemans Analytical X-ray Instrument Inc., Madison, Wisconsin, USA.

23 A. Altomare, M. C. Burla, M. Camalli, M. Cascarano, C. Giacovazzo, A. Guagliardi, and G. Polidori, *J. Appl. Crystallogr.*, **27**, 435 (1994).

24 P. T. Beurskens, G. Admiraal, G. Beurskens, W. P. Bosman, R. de Gelder, R. Israel, and J. M. M. Smits, "The DIRDIF Program System: Technical Report of the Crystallography Laboratory," University of Nijmegen, The Netherlands (1994).

25 Least-Squares: Function minimized: $\Sigma_w (|F_o| - |F_c|)^2$ where $w = 1/[\sigma^2(F_o)] = [\sigma_c{}^2 (F_o) + p^2 F_o{}^2/4]^{-1}$, $sc(F_o) =$ e.s.d. based on counting statistics, $p = p$-factor.

26 D. T. Cromer and J. T. Waber, "International Tables for X-ray Crystallography," The Kynoch Press, Birmingham, England (1974), Vol. IV, Table 2.2 A.

27 J. A. Ibers and W. C. Hamilton, *Acta Crystallogr.*, **17**, 781 (1964).

28 D. C. Creagh and W. J. McAuley, "International Tables for Crystallography," ed by A. J. C. Wilson, Kluwer Academic Publishers, Boston (1992), Vol. C, p. 219, Table 4.2.6.8.

29 D. C. Creagh and J. H. Hubbell, "International Tables for Crystallography," ed by A. J. C. Wilson, Kluwer Academic Publishers, Boston (1992), Vol. C, p. 200, Table 4.2.4.3.

30 teXsan: Crystal Structure Analysis Package, Molecular Structure Corporation (1985 & 1999).